Supplemental Document

Biomedical Optics EXPRESS

Measurement of arbitrary scan patterns for correction of imaging distortions in laser scanning microscopy: supplement

PATRICK ROSE, ALEXANDR KLIOUTCHNIKOV, DAMIAN J. WALLACE, DAVID S. GREENBERG, JASON N. D. KERR, AND JUERGEN SAWINSKI*

MPI f. Neorobiol. of Behavior – caesar, Ludwig-Erhard-Allee 2, 53175 Bonn, Germany
**juergen.sawinski@mpinb.mpg.de*

Supplement DOI: https://doi.org/10.6084/m9.figshare.19723312

Parent Article DOI: https://doi.org/10.1364/BOE.454155

Measurement of arbitrary scan patterns for correction of imaging distortions in laser scanning microscopy: supplemental document

In the following all necessary details to implement methods to extract a scan pattern from any laser scanning microscope are described.

1. Z-SCAN TECHNIQUE

The Z-scan technique[1] is a simple means to measure the axial point-spread function (PSF) in multi-photon-excitation (MPE) based microscopy. Here, a volumetric intensity profile is acquired along the z-axis (i.e. the optical axis) by recording fluorescent flux through an orthogonal plane separating a fluorescent and a non-fluorescent region. The axial PSF $\psi_p(z)$ of the emission[1] is related to the acquired intensity via

$$I(z) \propto \int_z^\infty \psi_p(\zeta - z_0)\,\mathrm{d}\zeta \tag{S1}$$

for p^{th}-order excitation (note, that for $p = 1$ the intensity $I(z)$ is constant), where z_0 was defined as an arbitrary offset determining the interface between fluorescent (in positive z-direction) and non-fluorescent probe. The actual profile can be recovered by differentiating the intensity profile $I(z)$ or fitting an appropriate function to the acquired data.

By tomographically scanning through several such interfaces this scheme can be extended to capture the volumetric PSF $\psi_p(\mathbf{z})$ for each pixel-wise detected focal volume but, more importantly, allows to retrieve the geometry (i.e. the three-dimensional shape) of the scan pattern contained in the z_0 essential for unambiguous reconstruction of anatomical features of the specimen under observation.

2. GEOMETRIC Z-SCAN

The geometric z-scan is executed in $\mathbb{R}^3$ along trajectories

$$\left(\mathbf{T}\right)_{nm}(z) \coloneqq \left(\mathbf{T}_0\right)_{nm} + z \cdot \left(\mathbf{t}^0\right)_n \tag{S2}$$

with the origin $\mathbf{T}_0$ and direction $\mathbf{t}^0$ through the interface plane

$$P_n : \left\{ \mathbf{x} \,\middle|\, \left(\mathbf{x} - \left(\mathbf{P}_0\right)_n\right) \cdot \left(\mathbf{p}^0\right)_n = 0 \right\}, \tag{S3}$$

with an arbitrary point $\mathbf{P}_0$ on the plane and it's surface normal $\mathbf{p}^0$ (see Fig. S1). Here, n is the plane index and m the interface-traversal per plane. The trajectory is commonly executed step-wise ($z(q) = z_q$, $q \in 0, 1, \ldots$) resulting in the image sequence

$$\left(I_{ij}\right)_{nm}(q) \coloneqq c_{nm} \cdot \int_{z(q)}^\infty \left(\psi_{p,ij}\right)_{nm}\Big(\left(\mathbf{T}\right)_{nm}(\zeta)\Big)\,\mathrm{d}\zeta \quad \text{with} \quad c_{nm} = \text{const} \tag{S4}$$

where I_{ij} is the pixel intensity for all indices i and j.[2] Assuming a near GAUSSIAN profile (see Sec. 3ff.)

$$\psi_p \propto \exp\left\{ -p \left(\frac{z - z_0}{\sigma} \right)^2 \right\} \tag{S5}$$

[1] In the following we will only deal with a normalized PSF, thus,

$$\psi_p(\mathbf{z}) = \frac{[\psi(\mathbf{z})]^p}{\langle [\psi(\mathbf{z})]^p \rangle},$$

where ψ is the PSF of the excitation beam (cf. Eq. S18).

[2] The proportionality constant in (S4) depends on pulse properties, order of effect, wavenlength, dye and dye concentration [2] and is expected to be constant at least during the scan of a single plane and trajectory.

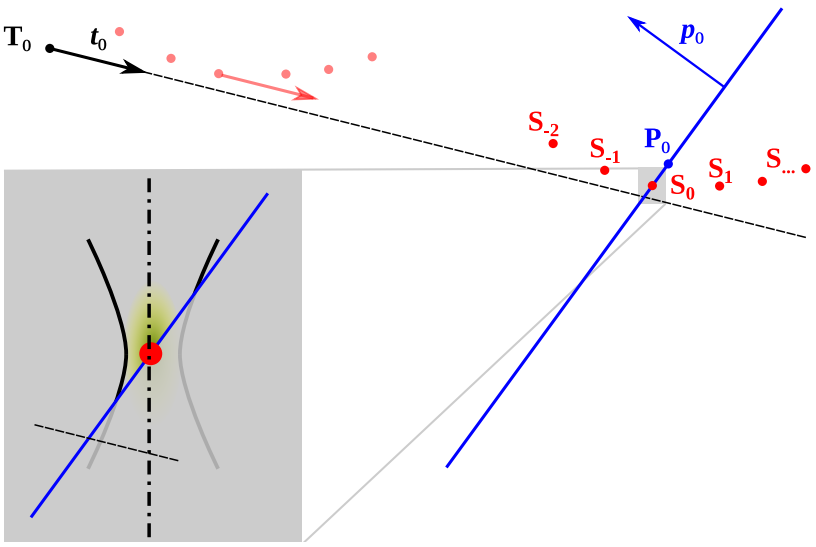

Fig. S1. Two-dimensional depiction of the precedure of scanning through an interface plane on a single trajectory. The plane P (blue) is defined by a point $\mathbf{P}_0$ and its surface normal $\mathbf{p}^0$ separating a fluorescent (left) and non-fluorescent (right) region. The individual points of the scan patter $\mathbf{S}_x$ (red) are shifted along the scan trajectory which is defined by its origin $\mathbf{T}_0$ and direction $\mathbf{t}_0$ (two arbirarily selected positions of the scan path are display). They magnified, shaded area (grey) portrays the GAUSSIAN beam shape with elicited fluorescence (green) for a selected pixel.

in any direction the individual transitions $(z_{0,ij})_{nm}$ can be recovered by, for example chi-square minimization, using the fit function

$$f(z_0, \sigma, A, I_0) := I_0 + \frac{A}{2}\left(1 + \operatorname{erf}\left\{-\frac{z - z_0}{\sigma}\right\}\right) \tag{S6}$$

for each pixel and trajectory individually, thus, the three-dimensional transistion coordinates are

$$(\mathbf{z}_{0,ij})_{nm} = (\mathbf{T}_0)_{nm} + (z_{0,ij})_{nm} \cdot (\mathbf{t}^0)_n \,. \tag{S7}$$

The actual, pixel-wise scan trajectory, though, is offset by the scan-pattern:

$$(\mathbf{T}_{ij})_{nm} \to (\mathbf{T})_{nm} + \mathbf{S}_{ij} \,, \tag{S8}$$

where the scan-pattern is defined by

$$S : \left(\mathbf{S}_{ij}, t_{ij}\right) \tag{S9}$$

with the spatial and temporal components $\mathbf{S}_{ij}$ and t_{ij}, respectively (in the following we will ignore the temporal components). The plane-trajectory intersection, thus, is

$$P_n \cap \left((\mathbf{T})_{nm} + \mathbf{S}_{ij}\right) = (\mathbf{z}_{0,ij})_{nm} \,, \tag{S10}$$

which can be written as a system of linear equations (see Eq. S3):

$$\left[(\mathbf{z}_{0,ij})_{nm} + \mathbf{S}_{ij} - (\mathbf{P}_0)_n\right] \cdot (\mathbf{p}^0)_n = 0 \,. \tag{S11}$$

Interface planes To first calculate the plane parameters, noting that $\mathbf{S}_{ij}$ does not depend on n and m, we may choose an appropriate origin of the scan path which may be a single or a range of pixels i and j, so that

$$\left\langle \mathbf{S}_{ij} \right\rangle = \mathbf{0} \,. \tag{S12}$$

Taking the same average over (S11) we may now select an arbitrary m for which

$$(\mathbf{P}_0)_n = (\bar{\mathbf{z}})_{nm} \quad \text{with} \quad \bar{\mathbf{z}} = \left\langle \mathbf{z}_{0,ij} \right\rangle \,. \tag{S13}$$

The respective interface normal is found using

$$\left(\mathbf{p}^0\right)_n = \frac{\left(\mathbf{p}\right)_n}{\left\langle \left(\mathbf{p}\right)_n \right\rangle} \quad \text{with} \quad \left(\mathbf{p}\right)_n = \left(\left(\bar{\mathbf{z}}_{m-1} - \bar{\mathbf{z}}_m\right) \times \left(\bar{\mathbf{z}}_{m+1} - \bar{\mathbf{z}}_m\right)\right)_n \tag{S14}$$

with indexes $m+1$ and $m-1$ (mod M), M being the number of interface traversals.

Scan pattern With the known interface planes P_n the scan pattern can now be infered (see Eq. S11) using

$$\mathbf{S}_{ij,m} = \frac{\left(\mathbf{p}^0\right)_n^{\mathrm{T}} \left[\left(\mathbf{P}_0\right)_n - \left(\mathbf{z}_{0,ij}\right)_{nm}\right]}{\left(\mathbf{p}^0\right)_n^{\mathrm{T}}} \,. \tag{S15}$$

The results for the individual m can be averaged, so that

$$\mathbf{S}_{ij} = \left\langle \mathbf{S}_{ij,m} \right\rangle_m \,. \tag{S16}$$

3. VOLUMETRIC Z-SCAN

As stated before the axial z-scan can be extended so that the volumetric PSF could be detected using tomographic reconstruction over the full FOV. However, optical aberrations can lead to very complex shapes of the PSF which would render a tomographic reconstruction of the focal volume inept [3].

For ordinary laser scanning microscopes, however, several reasonable assumptions can be made: 1. the excitation beam is quasi GAUSSIAN, 2. the optical system is well corrected to attain a minimal focus volume, and, 3. par-axial approximations apply.[3] In addition, effects such as beam truncation (cf. [5]) leading to an AIRY pattern, or, absorption and scattering (cf. [6]) are neglected.

Hence the PSF is described by

$$\psi_p(\rho,\zeta) \propto \left[\frac{1}{1+\zeta^2} \exp\left\{-\frac{\rho^2}{1+\zeta^2}\right\}\right]^p \tag{S17}$$

for p-th order MPE using normalized coordinates $\rho = |\mathbf{r}|/w_0$ and $\zeta = z/z_{\mathrm{R}}$, with the focal plane beam diameter w_0 and the RAYLEIGH range z_{R}.

4. ACCURACY

In this section the accuracy and deviations of the minimization using the error function (Eq. S6) due to differences in shape of transverse and axial behavior as well as the influence of the inherent shot-noise shall be reviewed. In addition the last paragraph will consider influences due to reflections in the probe.

A. Shape dependence

For further considerations we use the normalization

$$\lim_{z\to\pm\infty} \psi_p(z) = 0\,, \quad \langle \psi_p(z) \rangle = 1\,, \quad \langle z\psi_p(z) \rangle = 0\,, \text{ and } \psi_p(0.5) = 0.5 \cdot \psi_p(0)\,, \tag{S18}$$

which means, that 1. $I(z) \in [0,1]$, 2. the expected transition z_0 relates to $\psi_p(0)$ (centroid), and, 3. the full-width-half-maximum (FWHM) is 1.

The acquired intensity distribution (see Eqs. S4, S17) thus stems from a mixture between the transverse

$$\psi_{p,\text{transverse}}(r) = \frac{p}{2\sqrt{\pi}\sqrt{\log 2}} \exp\left\{-4\,\log 2 \cdot r^2\right\} \tag{S19}$$

and par-axial

$$\psi_{p,\text{axial}}(z) = \frac{2\beta}{\sqrt{\pi}} \frac{\Gamma(p)}{\Gamma\left(p-\frac{1}{2}\right)} \frac{1}{(1+4\beta^2 z^2))^p} \quad \text{with} \quad \beta = \sqrt{2^{\frac{1}{p}}-1} \tag{S20}$$

shape of the PSF.

[3] High numerical aperture optics will require higher-order corrections to the transverse GAUSSIAN shape of the excitation beam [4].

With the normalization introduced above the fit function (Eq. S6) becomes

$$f(\sigma) = \frac{1}{2}\left(1 + \operatorname{erf}\left\{-\frac{z}{\sigma}\right\}\right) \tag{S21}$$

To first order any sigmoidal function is dominated by the slope near the point of symmetry, so that for any bell-shaped PSF ψ (normalized according to Eq. S18) we yield

$$\frac{\partial}{\partial z} f\Big|_{z=0} = \frac{1}{\sigma\sqrt{\pi}} = \psi(0)\,. \tag{S22}$$

As the FWHM is commonly used as criterion for optical resolution in laser scanning microscopy, we may also state that, according to (S18) the FWHM is the inverse of the width parameter in (S21):

$$\sigma_{\mathrm{FWHM}} = \sigma^{-1} = \sqrt{\pi}\psi(0)\,. \tag{S23}$$

Transverse For the GAUSSIAN PSF

$$\psi_{p,\mathrm{transverse}}(0) = \frac{p}{2\sqrt{\pi}\sqrt{\log 2}} \tag{S24}$$

the FWHM is unsurprisingly $\sigma_{\mathrm{FWHM}} = 2\sqrt{\log 2} \approx 1.665$ and the intensity contained within the interval $[-\sigma, \sigma]$ is $\operatorname{erf}(1) \approx 84.3\%$.

Par-axial For the par-axial PSF

$$\psi_{p,\mathrm{axial}}(0) = \frac{2\beta}{\sqrt{\pi}} \frac{\Gamma(p)}{\Gamma\left(p - \frac{1}{2}\right)} \quad \text{with} \quad \beta = \sqrt{2^{\frac{1}{p}} - 1} \tag{S25}$$

the FWHM is $\sigma_{\mathrm{FWHM},2} \approx 1.452$ and $\sigma_{\mathrm{FWHM},3} \approx 1.534$ and the intensity contained within the interval $[-\sigma, \sigma]$ is 77.8% and 80.3% for 2- and 3-photon excitation, respectively.

From this we conclude that the error function given in (S6) is well suited as fit function.

B. Reflection

For the construction of the test sample we had used high quality microscope slides, which, depending on the angle of incidence α, have a FRESNEL reflection coefficient

$$r_\perp = \frac{\cos\alpha - \sqrt{n^2 - \sin^2\alpha}}{\cos\alpha + \sqrt{n^2 - \sin^2\alpha}} \quad \text{with} \quad n = \frac{n_2}{n_1} \tag{S26}$$

for s-polarization with the incidence and transmission volume refractive indices n_1 and n_2 (note that for the coefficient for p-polarization $r_\parallel \leq r_\perp$ applies). With this we can estimate the upper limit of relative excitation efficiency as

$$\Delta I_p \leq r^{2p} \tag{S27}$$

with the excitation order p. With the refractive indices $n_1 = 1.33$ for water and $n_2 = 1.51$ for glass the influence is negligible (see Fig. S2).

REFERENCES

1. M. Sheik-Bahae, A. Said, T.-H. Wei, D. Hagan, and E. Van Stryland, "Sensitive measurement of optical nonlinearities using a single beam," IEEE J. Quantum Electron. **26**, 760–769 (1990).
2. J. B. Pawley and B. R. Masters, "Handbook of Biological Confocal Microscopy, Third Edition," J. Biomed. Opt. **13**, 029902 (2008).
3. R. M. Mersereau, "Digital reconstruction of multidimensional signals from their projections." Ph.D. thesis, Massachusetts Institute of Technology (1973).
4. G. P. Agrawal and D. N. Pattanayak, "Gaussian beam propagation beyond the paraxial approximation," JOSA **69**, 575–578 (1979).
5. V. N. Mahajan, "Uniform versus Gaussian beams: a comparison of the effects of diffraction, obscuration, and aberrations," JOSA **3**, 470–485 (1986).
6. P. Theer and W. T. Denk, "On the fundamental imaging-depth limit in two-photon microscopy," in *Femtosecond Laser Applications in Biology*, vol. 5463 S. Avrillier and J.-M. Tualle, eds., International Society for Optics and Photonics (SPIE, 2004), pp. 45 – 55.

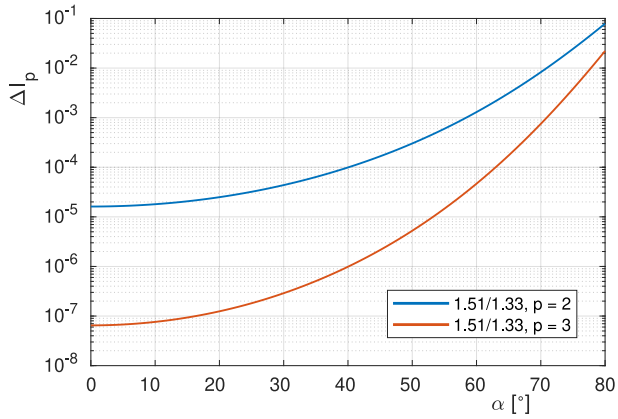

Fig. S2. Relative intensity of MPE due to reflection at a glass surface immersed in water calculated for two- and three-photon excitation.